

Cite this: *Catal. Sci. Technol.*, 2018, 8, 2061

Received 11th January 2018,  
Accepted 16th March 2018

DOI: 10.1039/c8cy00073e

[rsc.li/catalysis](http://rsc.li/catalysis)

$M^1[Co(CN)_6]_{2/3}$ -type Prussian blue analogues (M<sup>1</sup>-Co PBAs) were studied as catalysts for the synthesis of propargylamines *via* A<sup>3</sup> coupling of phenylacetylene, benzaldehyde and piperidine.  $Cu_{0.8}Zn_{0.14}$ -Co PBA was the best catalyst for the reaction by combining the high conversion obtained with Cu-Co PBA with the excellent selectivity obtained with Zn-Co PBA.

The reaction between a terminal alkyne, a secondary amine and an aldehyde, also known as the A<sup>3</sup> coupling, is a multicomponent reaction with a high atom efficiency and water as the only by-product. Therefore, it is considered a green process for the synthesis of pharmaceutical intermediates or final products such as bioactive propargylamines.<sup>1–5</sup> In order to carry out the reaction in substantially short times and with high selectivity to the propargylamine product (the A<sup>3</sup> product) the use of a catalyst – normally containing transition metals – is necessary.<sup>6–12</sup> To simplify catalyst recovery, heterogenization of the active phase is desired.<sup>6,13–17</sup>

Prussian blue analogues (PBAs), in many cases also referred to as double metal cyanides (DMCs), are cyanide-bridged transition metal coordination polymers with the general formula  $M^1_u[M^2(CN)_6]_v \cdot xH_2O$  (hereafter abbreviated as ‘M<sup>1</sup>-M<sup>2</sup> PBA’). PBAs are easily synthesized by a precipitation reaction between aqueous solutions of the cyanometalate complex,  $[M^2(CN)_6]^{u-}$ , and an M<sup>1</sup> salt.<sup>18</sup> Even though PBAs were among the first reported coordination polymers, their use as catalyst only dates back to the 1960s.<sup>18</sup> Recently, several studies have focused on the expansion of the catalytic applications of PBAs. This can be achieved by virtue of the multiple possible variations in the active metal as well as by

Centre for Surface Chemistry and Catalysis, KU Leuven, Celestijnenlaan 200F, 3001 Leuven, Belgium. E-mail: [dirk.devos@kuleuven.be](mailto:dirk.devos@kuleuven.be), [trees.debaerdemaeker@kuleuven.be](mailto:trees.debaerdemaeker@kuleuven.be)

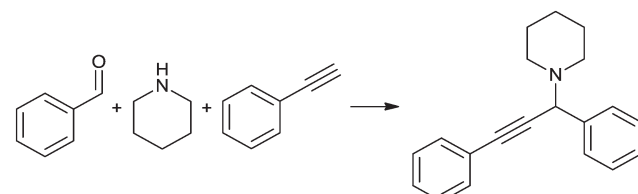
† Electronic supplementary information (ESI) available: Experimental details (synthesis of the PBAs, characterization, catalytic testing), additional characterization (ICP, high resolution XRD patterns and Pawley fitting, N<sub>2</sub> physisorption isotherms) and catalytic data. See DOI: [10.1039/c8cy00073e](https://doi.org/10.1039/c8cy00073e)

## Tunable Prussian blue analogues for the selective synthesis of propargylamines through A<sup>3</sup> coupling†

Carlos Marquez, Francisco G. Cirujano, Cédric Van Goethem, Ivo Vankelecom, Dirk De Vos \* and Trees De Baerdemaeker \*

changes in synthesis procedures (e.g. using alcohols and other organic additives). For example, Zn-Co PBA based materials are well-known epoxide polymerization catalysts<sup>19,20</sup> and have also been used as catalyst for the activation of alkynes in hydroamination reactions (C–N bond formation),<sup>21</sup> and for copolymerization of CO<sub>2</sub> and epoxides.<sup>22,23</sup> Moreover, mixed metal PBAs (Fe<sup>2+</sup>,Cu<sup>2+</sup>-Co PBA) have been employed as solid catalysts for the aerobic oxidation of oximes to carbonyl compounds.<sup>24</sup> In this work, we have synthesized a series of PBAs based on earth-abundant divalent metals (Fe, Co, Ni, Cu and Zn) and investigated their potential for the synthesis of propargylamines *via* C–H activation in the A<sup>3</sup> coupling reaction of phenylacetylene, benzaldehyde and piperidine (Scheme 1). To the best of our knowledge, this is the first time that PBAs are applied for C–H activation of phenylacetylene in multicomponent reactions.

A series of PBAs were synthesized by modifying previously reported procedures<sup>25,26</sup> through addition of an aqueous solution of K<sub>3</sub>[Co(CN)<sub>6</sub>] to an aqueous solution of a M<sup>1</sup>Cl<sub>2</sub>·xH<sub>2</sub>O salt (FeCl<sub>2</sub>·4H<sub>2</sub>O, CoCl<sub>2</sub>, NiCl<sub>2</sub>·6H<sub>2</sub>O, CuCl<sub>2</sub>·2H<sub>2</sub>O or ZnCl<sub>2</sub>) containing PTMEG and *tert*-butanol. ICP analyses of selected PBA samples show that the M<sup>1</sup>/Co ratio obtained is higher than the stoichiometric 1.5, indicating that a slight excess of M<sup>1</sup> is present in the structure (Table S1†). This is expected, considering that with a 10 to 1 ratio M<sup>1</sup>Cl<sub>2</sub>·xH<sub>2</sub>O to K<sub>3</sub>[Co(CN)<sub>6</sub>], an excess M<sup>1</sup>Cl<sub>2</sub>·xH<sub>2</sub>O was used during the synthesis. The crystallinity of the samples was confirmed by powder X-ray diffraction (PXRD, Fig. S1†). All samples show



**Scheme 1** A<sup>3</sup> coupling between phenylacetylene, benzaldehyde and piperidine to produce the corresponding propargylamine.



reflections corresponding to a cubic phase typical for metal hexacyanocobaltates.<sup>27–29</sup> As expected for the different  $M^1$ 's, the FTIR spectra of the samples show a blue shift in the position of the CN stretching band compared to  $K_3[Co(CN)_6]$  (Fig. S2†).<sup>26,30,31</sup> The textural properties of the PBAs vary depending on  $M^1$ , as evidenced by  $N_2$  physisorption (Table S2 and Fig. S3†). Although this type of material is usually microporous in nature, the  $N_2$  isotherms of Fe–Co, Co–Co and Cu–Co PBA also exhibit a hysteresis loop around  $p/p_0 = 0.8$ , indicative of the presence of mesopores. The acid properties of selected samples were studied with pyridine adsorption followed by FTIR spectroscopy (Fig. S4 and Table S2†). The bands at 1450, 1490 and 1610  $cm^{-1}$  are attributed to pyridine adsorbed on Lewis acid sites.<sup>32</sup> No band was observed around 1540  $cm^{-1}$ , which indicates that there are no Brønsted acid sites in the samples.<sup>32</sup>

All synthesized PBA samples were investigated both in terms of activity and selectivity to the  $A^3$  product. The reaction rate was particularly sensitive to the nature of the  $M^1$  metal (Fig. 1 and S5†). For the bimetallic  $M^1$ –Co PBAs, the highest reaction rate was obtained with Cu–Co PBA, exhibiting an activity one order of magnitude higher than the other PBAs. These results are in line with the reported excellent catalytic activity of Cu sites for this type of reaction.<sup>14–17,33,34</sup> In the case of Fe–Co PBA, the activity for the  $A^3$  coupling reaction was low and the predominant reaction was the reduction of benzaldehyde to benzyl alcohol, most likely following a Meerwein–Ponndorf–Verley (MPV) mechanism due to the presence of 2-butanol as solvent and potential reductant. Even though the use of Fe as catalytic site has been reported for both  $A^3$  coupling and MPV reactions,<sup>12,35,36</sup> this specific Fe site favors the reduction of benz-

aldehyde over the C–H activation of phenylacetylene under these reaction conditions (Fig. S6†).

On the one hand, the highest phenylacetylene conversion was obtained with Cu–Co PBA (Fig. 1). On the other hand, the selectivity towards the  $A^3$  product was higher using Zn–Co PBA compared to the other metals. In the latter case, just a small amount of acetophenone was produced. This trend is also maintained when the selectivity is assessed at the same phenylacetylene conversion (Fig. S7†). In light of this, a series of  $Cu_xZn_{1-x}$ –Co multi-metal PBA complexes with different Cu/Zn ratios was prepared with the aim of tuning the catalytic performance of the system.

Elemental analysis showed that the multi-metal samples,  $Cu_xZn_{1-x}$ –Co PBA, contain a much larger amount of Cu than Zn, compared to the initial Cu/Zn molar ratios used during synthesis (Table S1†). High resolution X-ray diffraction measurements and Pawley fitting (Fig. S8†) allowed the refinement of the lattice parameters of the sample  $Cu_{0.86}Zn_{0.14}$ –Co PBA, which was found to crystallize in the cubic space group  $Fm\bar{3}m$  – just like Cu–Co PBA and Zn–Co PBA (Fig. S9 and S10†). As expected given the high Cu content, the lattice parameters of  $Cu_{0.86}Zn_{0.14}$ –Co PBA are in between those of Cu–Co PBA and Zn–Co PBA, but much closer to those of Cu–Co PBA (Table S3†). Similarly, the rest of the multi-metal samples show reflections corresponding to a cubic phase (Fig. S11†). Other physicochemical properties of the multi-metal samples ( $\nu(C\equiv N)$ , Lewis acidity, textural properties) are also intermediate between those of Cu–Co PBA and Zn–Co PBA (Table S2 and Fig. S3, S4 and S12†). Furthermore, HAADF-STEM images (Fig. 2) of the sample  $Cu_{0.86}Zn_{0.14}$ –Co PBA confirm the formation of a single PBA phase and the close

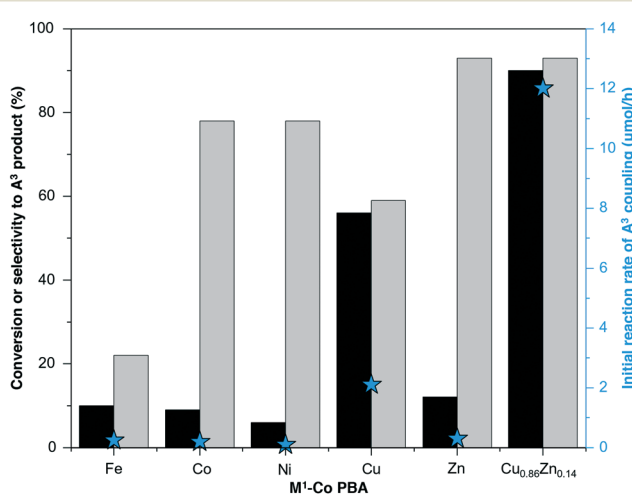


**Fig. 1** Conversion (■) and selectivity (▨) to the  $A^3$  product for the coupling of phenylacetylene (0.05 mmol), piperidine (0.1 mmol) and benzaldehyde (0.1 mmol) after 24 h reaction time at 383 K and initial rate (★) of the  $A^3$  coupling expressed as  $\mu\text{mol}$  of  $A^3$  product formed per h over 10 mg of PBA. Conversion and selectivity are based on phenylacetylene. Acetophenone was the only phenylacetylene-derived side-product detected.

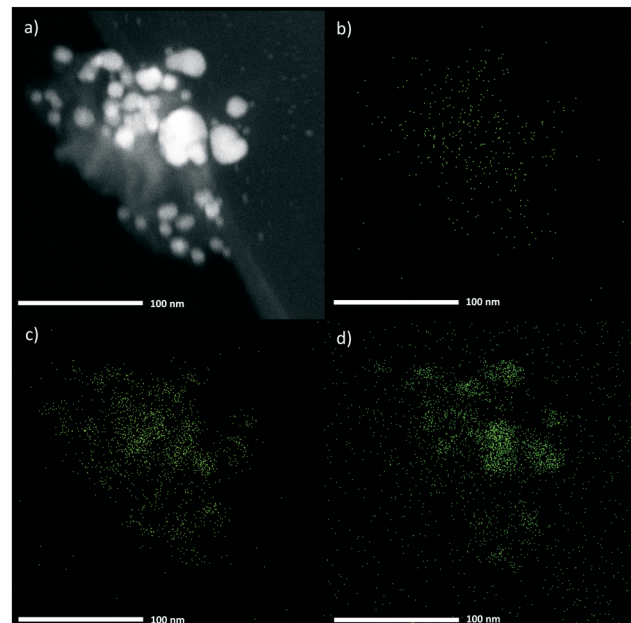


**Fig. 2** HAADF-STEM image (a) and EDX composition mapping for Zn (b), Co (c) and Cu (d) of the sample  $Cu_{0.86}Zn_{0.14}$ –Co PBA.



proximity between Zn and Cu, as no segregated Zn-rich or Cu-rich phases are observed.

The incorporation of Cu into the Zn-Co PBA increased the catalytic activity of the solid for the  $A^3$  coupling reaction in comparison to the original Zn-Co PBA (Fig. 3). Remarkably, at higher Cu content, the simultaneous presence of Cu and Zn in the structure yielded catalysts exhibiting activity superior to that of Cu-Co PBA. In fact, the TOF obtained with the most active multi-metal sample ( $Cu_{0.86}Zn_{0.14}$ -Co PBA) was almost five times higher than the one obtained with Cu-Co PBA (Table 1). This suggests a synergistic effect when combining Zn and Cu in the same crystalline framework. Furthermore, the selectivity to the  $A^3$  product is also increased with respect to the Cu-Co PBA, from 60% to 93% at 90% conversion of phenylacetylene (Fig. S7†). This increase is attributed to the presence of Zn sites in the PBA structure: they could facilitate the formation of the iminium ion, while also helping in the C-C bond formation between the iminium ion and the Cu-coordinated alkyne (Scheme 2).<sup>37</sup>

To further prove this hypothesis, additional reactions were performed first in the absence of, and then with only phenylacetylene in the reaction mixture (Table 1). Results show that  $Zn^{2+}$  sites seem to facilitate the coupling between benzaldehyde and piperidine to form  $\alpha$ -phenyl-1-piperidinemethanol and 1-benzylpiperidine, with Zn-Co PBA exhibiting a TOF almost double the TOF of Cu-Co PBA for this reaction. The product 1-benzylpiperidine is believed to be formed by reduction of the iminium ion *via* a hydrogen-transfer mechanism involving the 2-butanol solvent.<sup>38</sup> In contrast, Cu sites appear to enable the activation of phenylacetylene. The TOF obtained with the Cu-Co PBA was two orders of magnitude higher than the one obtained with Zn-Co PBA for the hydration of phenylacetylene. Contrary to previous reports<sup>13,39</sup> claiming that the formation of the iminium ion between the aldehyde and the amine occurs almost spontaneously above

**Table 1** TOF ( $h^{-1}$ ) in the  $A^3$  coupling reaction and in additional test reactions for selected  $M^1$ -Co PBA samples

	Cu	Zn	$Cu_{0.86}Zn_{0.14}$
TOF $A^3$ coupling <sup>a</sup>	0.43	0.052	2.1
TOF phenylacetylene hydration <sup>b</sup>	0.18	0.0025	0.055
TOF benzaldehyde-piperidine coupling <sup>c</sup>	0.24	0.43	0.40

<sup>a</sup> Turnover frequency based on initial rates of the  $A^3$  coupling reaction expressed as mmol of  $A^3$  product formed per mmol of  $M^1$  (Cu, Zn or Cu + Zn) per h. <sup>b</sup> Turnover frequency for the hydration of phenylacetylene (0.05 mmol) at 383 K for 6 h expressed as mmol of acetophenone formed per mmol of  $M^1$  (in the absence of piperidine and benzaldehyde) per h. <sup>c</sup> Turnover frequency for the piperidine (0.05 mmol) and benzaldehyde (0.05 mmol) coupling at 383 K for 24 h expressed as mmol of 1-benzylpiperidine and  $\alpha$ -phenyl-1-piperidinemethanol formed per mmol of  $M^1$  in the absence of phenylacetylene per h.

353 K, our results show that a specific site –  $Zn^{2+}$  in this case – is needed for this reaction to occur considerably. Without Zn, the rapid activation of phenylacetylene (on Cu sites) yields considerable amounts of acetophenone, whereas without Cu in the structure, this activation takes place too slowly and the coupling of phenylacetylene, piperidine and benzaldehyde does not occur substantially. Blank experiments of the reactions under the same conditions did not produce detectable amounts of any product, also confirming this hypothesis.

Moreover, the selectivity to the  $A^3$  product was very different when the Cu active sites were in the form of soluble species (Table S4†). In the case of the homogeneous  $Cu(OAc)_2$ ,  $CuCl_2$  and  $Cu(ClO_4)_2$  catalysts, only 1,4-diphenylbuta-1,3-diyne (from the homocoupling of phenylacetylene) was detected as a product after 24 h, which is not formed when PBAs are used as catalyst. This result suggests that under these reaction conditions, the  $Cu^{2+}$  centers in the PBA framework are stable and maintain their +2 oxidation state.<sup>15</sup> Additionally,  $Cu_{0.86}Zn_{0.14}$ -Co PBA exhibited a similar selectivity and a higher conversion than the homogenous  $ZnCl_2$  salt. A comparable activity was obtained with respect to other heterogeneous Cu-containing catalysts reported in literature, such as of  $[Cu(2-pymo)_2]$  and Cu nanoparticles supported on graphene under similar reaction conditions.<sup>15,40</sup> In aprotic solvents (both non polar like toluene and dioxane, and polar and highly coordinating such as DMSO) the yields of the  $A^3$  product decreased (Table S5†). The best catalytic performance of the  $Cu_{0.86}Zn_{0.14}$ -Co PBA was obtained with 2-butanol as a solvent at 383 K. Protic, polar solvents have been found to improve the rate of  $A^3$  coupling reaction, presumably by facilitating initial iminium ion formation due to the stabilization of charged activation states.<sup>41</sup>

The yield of  $A^3$  product *vs.* time is plotted in Fig. S13† for  $Cu_{0.86}Zn_{0.14}$ -Co PBA. The kinetics of the  $A^3$  coupling reaction are still a matter of debate. It has been reported that the phenylacetylene conversion *vs.* time plot should follow a trend similar to pseudo second-order kinetics because the production of the propargylamine depends on the

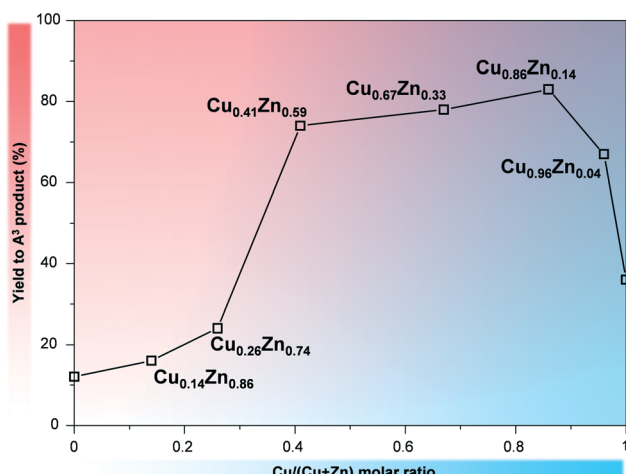
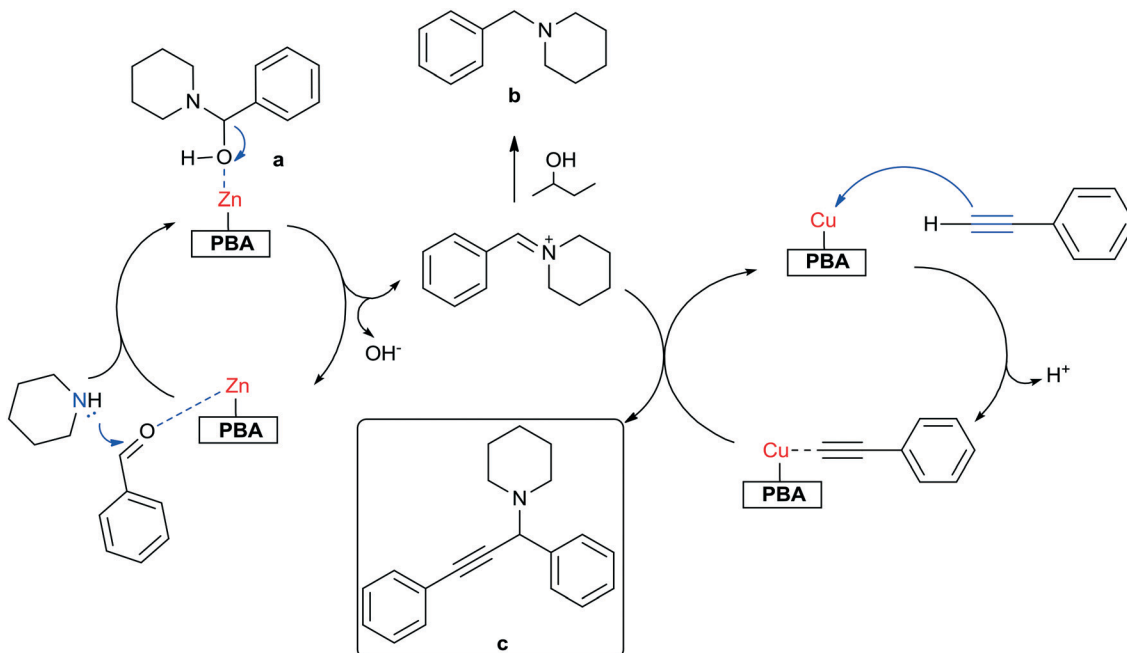


**Fig. 3** Yield of  $A^3$  product after 24 h reaction time for the coupling of phenylacetylene (0.05 mmol), piperidine (0.1 mmol) and benzaldehyde (0.1 mmol) at 383 K over 10 mg of  $Cu_xZn_{1-x}$ -Co PBA with different Cu/(Cu + Zn) molar ratios.





**Scheme 2** Proposed reaction mechanism for the  $A^3$  coupling reaction of phenylacetylene, piperidine and benzaldehyde catalyzed by a  $Cu_xZn_{1-x}$ -Co multi-metal PBA. **a** =  $\alpha$ -phenyl-1-piperidinemethanol, **b** = 1-benzylpiperidine, **c** =  $A^3$  product (1-(1,3-diphenyl-2-propyn-1-yl)piperidine).

concentration of both phenylacetylene and the iminium ion.<sup>15</sup> However, more recent studies fitted the data by a first-order kinetics equation with respect to phenylacetylene.<sup>42</sup> Analysis of the conversion of phenylacetylene at different reaction times reveals that the best fit (highest coefficient of determination,  $R^2$ ) was obtained when the data were fitted by first-order in the alkyne (Fig. S14†). This result was further supported by the evaluation of the variation of the reaction rate with respect to the concentration of phenylacetylene (Fig. S15†). When the concentration of phenylacetylene was doubled, the rate of the reaction also doubled, which suggests that the reaction order with respect to this reactant is equal to one. In contrast, when the concentration of piperidine was varied instead (Fig. S16†), a lower reaction rate for the  $A^3$  coupling was observed as the initial concentration of piperidine was increased. This not only shows that the reaction order is not equal to one with respect of piperidine, but also suggests inhibition caused by piperidine due to strong adsorption on  $Cu^{2+}$  sites or formation of  $Cu$  complexes.<sup>43–47</sup>

Finally, the heterogeneity of the catalyst was studied by a hot filtration test. As shown in Fig. S17,† the hot filtrate shows no appreciable activity after stirring for an additional 20 h, indicating that there is no leaching of active species from the catalyst. This was further corroborated by elemental analyses performed after reaction (Table S1†). Remarkably, recycling tests show that  $Cu_{0.86}Zn_{0.14}$ -Co PBA largely maintains its activity after five runs (80% yield after fifth run *vs.* 85% for the fresh catalyst), even though there is a phase change when compared to the pristine sample (Fig. S17†). However, no notable changes were observed in the FTIR spectrum of  $Cu_{0.86}Zn_{0.14}$ -Co PBA after one reaction cycle (Fig. S18†).

## Conclusions

The catalytic performance of a series of PBAs was evaluated for the synthesis of propargylamines through  $A^3$  coupling. These materials show the possibility of tuning their catalytic performance by virtue of the multiple possible variations in the active metal. Here, the combination of Zn and Cu yielded a series of synergistic  $Cu_xZn_{1-x}$ -Co multi-metal PBA complexes, with  $Cu_{0.86}Zn_{0.14}$ -Co PBA proving to be an active, selective and recyclable heterogeneous catalyst for the reaction.

## Conflicts of interest

There are no conflicts to declare.

## Acknowledgements

This project has received funding from the European Union's Horizon 2020 research and innovation programme under the Marie Skłodowska-Curie grant agreement No. 641887 (project acronym: DEFNET). F. G. C. acknowledges the European Union's Horizon 2020 research and innovation programme under the Marie Skłodowska-Curie grant agreement No. 750391 (project acronym SINMOF) for financial support. F. W. O. Vlaanderen (Research Foundation Flanders) is thanked for project funding (D. D. V.: research projects; C. V. G. and I. V.: grant no. G.0256.14N) and a Postdoctoral Fellowship (T. D. B.). D. D. V. thanks KU Leuven for the Metusalem grant CASAS. Funding for the TEM through Hercules project AKUL/13/19 is kindly acknowledged. The authors are grateful to prof. Andrew L. Goodwin, Hanna L. B. Boström, Emily M. Reynolds (University of Oxford) and the beamline staff of I11 (Diamond



Light Source) for collecting the high resolution XRD data during Block Allocation Group beamtime (EE13284). The authors thank Michael T. Wharmby (DESY) for useful discussions and prof. Jin Won Seo (KU Leuven) for TEM support.

## References

- 1 C. Wei and C.-J. Li, *J. Am. Chem. Soc.*, 2003, **125**, 9584–9585.
- 2 J. Dulle, K. Thirunavukkarasu, M. C. Mittelmeijer-Hazeleger, D. V. Andreeva, N. Raveendran Shiju and G. Rothenberg, *Green Chem.*, 2013, **15**, 1238–1243.
- 3 V. A. Peshkov, O. P. Pereshivko and E. V. Van der Eycken, *Chem. Soc. Rev.*, 2012, **41**, 3790–3807.
- 4 S. Sarkar, A. Banerjee and B. K. Patel, in *Multicomponent Reactions: Synthesis of Bioactive Heterocycles*, ed. K. L. Ameta and A. Dandia, CRC Press, Boca Raton, 2017, ch. 6, pp. 139–182.
- 5 W.-J. Yoo, L. Zhao and C.-J. Li, *Aldrichimica Acta*, 2011, **44**, 43–54.
- 6 S. Cheng, N. Shang, C. Feng, S. Gao, C. Wang and Z. Wang, *Catal. Commun.*, 2017, **89**, 91–95.
- 7 S. Sakaguchi, T. Mizuta, M. Furuwan, T. Kubo and Y. Ishii, *Chem. Commun.*, 2004, 1638–1639.
- 8 L. C. Akullian, M. L. Snapper and A. H. Hoveyda, *Angew. Chem., Int. Ed.*, 2003, **42**, 4244–4247.
- 9 Y. Kuninobu, Y. Inoue and K. Takai, *Chem. Lett.*, 2006, **35**, 1376–1377.
- 10 K. Namitharan and K. Pitchumani, *Eur. J. Org. Chem.*, 2010, **3**, 411–415.
- 11 W.-W. Chen, H.-P. Bi and C.-J. Li, *Synlett*, 2010, **3**, 475–479.
- 12 W.-W. Chen, R. V. Nguyen and C.-J. Li, *Tetrahedron Lett.*, 2009, **50**, 2895–2898.
- 13 T. R. Mandlimath and K. I. Sathyanarayanan, *RSC Adv.*, 2016, **6**, 3117–3125.
- 14 M. Gholinejad, F. Saadati, S. Shaybanizadeh and B. Pulkilathadathil, *RSC Adv.*, 2016, **6**, 4983–4991.
- 15 I. Luz, F. X. Llabrés i Xamena and A. Corma, *J. Catal.*, 2012, **285**, 285–291.
- 16 G. H. Dang, H. Q. Lam, A. T. Nguyen, D. T. Le, T. Truong and N. T. S. Phan, *J. Catal.*, 2016, **337**, 167–176.
- 17 P. Rania, P. F. Siril and R. Srivastava, *Mol. Catal.*, 2017, **433**, 100–110.
- 18 P. Valveckens and D. De Vos, in *New Materials for Catalytic Applications*, ed. V. I. Parvulescu and E. Kemnitz, Elsevier, Amsterdam, 2016, ch. 1, pp. 1–12.
- 19 J. Milgrom, *US Pat.*, 3278457, 1966.
- 20 R. J. Herold, *US Pat.*, 3278457, 1966.
- 21 A. Peeters, P. Valveckens, R. Ameloot, G. Sankar, C. E. A. Kirschchock and D. De Vos, *ACS Catal.*, 2013, **3**, 597–607.
- 22 X. H. Zhang, S. Chen, X. M. Wu, X. K. Sun, F. Liu and G. R. Qi, *Chin. Chem. Lett.*, 2007, **18**, 887–890.
- 23 J. Sebastian and D. Srinivas, *Appl. Catal., A*, 2014, **482**, 300–308.
- 24 A. García-Ortiz, A. Grirrane, E. Reguera and H. García, *J. Catal.*, 2014, **311**, 386–392.
- 25 C. Marquez, M. Rivera-Torrente, P. P. Paalanen, B. M. Weckhuysen, F. G. Cirujano, D. De Vos and T. De Baerdemaecker, *J. Catal.*, 2017, **354**, 92–99.
- 26 I. Kim, J. T. Ahn, C.-S. Ha, C. S. Yang and I. Park, *Polymer*, 2003, **44**, 3417–3428.
- 27 D. F. Mullica, W. O. Milligan, G. W. Beall and W. L. Reeves, *Acta Crystallogr., Sect. B: Struct. Crystallogr. Cryst. Chem.*, 1978, **34**, 3558–3561.
- 28 A. Ludi, H. U. Guedel and M. Ruegg, *Inorg. Chem.*, 1970, **9**, 2224–2227.
- 29 G. W. Beall, W. O. Milligan, J. Korp and I. Bernal, *Inorg. Chem.*, 1997, **16**, 2715–2718.
- 30 X.-H. Zhang, Z.-J. Huab, S. Chenc, F. Liua, X.-K. Suna and G.-R. Qi, *Appl. Catal., A*, 2007, **325**, 91–98.
- 31 J. Fernandez Bertran, J. Blanco Pascual and E. Reguera Ruiz, *Acta Crystallogr., Sect. A: Found. Crystallogr.*, 1990, **46**, 685–689.
- 32 E. P. Perry, *J. Catal.*, 1963, **2**, 371–379.
- 33 M. J. Albaladejo, F. Alonso, Y. Moglie and M. Yus, *Eur. J. Org. Chem.*, 2012, **16**, 3093–3104.
- 34 M. J. Albaladejo, F. Alonso and M. J. González-Soria, *ACS Catal.*, 2015, **5**, 3446–3456.
- 35 D. Schröder and H. Schwarz, *Angew. Chem., Int. Ed. Engl.*, 1990, **29**, 910–912.
- 36 A. Naik, T. Maji and O. Reiser, *Chem. Commun.*, 2010, **46**, 4475–4477.
- 37 R. R. Mondal, S. Khamarui and D. K. Maiti, *ACS Omega*, 2016, **1**, 251–263.
- 38 A. Peeters, L. Claes, I. Geukens, I. Stassen and D. De Vos, *Appl. Catal., A*, 2014, **469**, 191–197.
- 39 S. B. Park and H. Alper, *Chem. Commun.*, 2005, 1315–1317.
- 40 S. Frindy, A. El Kadib, M. Lahcini, A. Primo and H. García, *Catal. Sci. Technol.*, 2016, **6**, 4306–4317.
- 41 G. A. Price, A. K. Brisdon, K. R. Flower, R. G. Pritchard and P. Quayle, *Tetrahedron Lett.*, 2014, **55**, 151–154.
- 42 Q. Li, A. Das, S. Wang, Y. Chen and R. Jin, *Chem. Commun.*, 2016, **52**, 14298–14301.
- 43 C.-M. Fu and A. M. Schaffer, *Ind. Eng. Chem. Prod. Res. Dev.*, 1985, **24**, 68–75.
- 44 R. T. Pflaum and W. W. Brandt, *J. Am. Chem. Soc.*, 1954, **76**, 6215–6219.
- 45 P. Lahtinen, E. Lankinen, M. Leskelä and T. Repo, *Appl. Catal., A*, 2005, **295**, 177–184.
- 46 N. Zhao, L. Liu, F. Wang, J. Li and W. Zhang, *Adv. Synth. Catal.*, 2014, **356**, 2575–2579.
- 47 X. Qi, R. Bai, L. Zhu, R. Jin, A. Lei and Y. Lan, *J. Org. Chem.*, 2016, **81**, 1654–1660.

